



Structural identification of $Zn_xZr_yO_z$ catalysts for Cascade aldolization and self-deoxygenation reactions

Rebecca A.L. Baylon^a, Junming Sun^{a,*}, Libor Kovarik^{b,c}, Mark Engelhard^{b,c}, Houqian Li^a, Austin D. Winkelman^a, Yong Wang^{a,b,*}

^a The Gene & Linda Voiland School of Chemical Engineering and Bioengineering, Washington State University, Pullman, WA 99164, USA

^b Institute for Integrated Catalysis, Pacific Northwest National Laboratory, Richland, WA 99352, USA

^c Environmental Molecular Sciences Laboratory, Pacific Northwest National Laboratory, Richland, WA 99352, USA

ARTICLE INFO

Keywords:

Lewis acid-base pairs

Aldolization

Ketonization

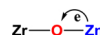
Mixed-Metal oxide

Oxygenates

Olefins

ABSTRACT

Complementary characterizations, such as nitrogen sorption, X-ray diffraction (XRD), X-ray photoelectron spectroscopy (XPS), visible Raman, scanning transmission electron microscopy (STEM) coupled with elemental mapping, NH_3/CO_2 temperature programmed desorption (NH_3/CO_2 -TPD), infrared spectroscopic analysis of adsorbed pyridine (Py-IR), and CO_2 -IR, have been employed to identify the structure and surface chemistry (i.e., acid-base) of mixed $Zn_xZr_yO_z$ oxide catalysts of varied ratios of Zn/Zr. Atomically dispersed Zn^{2+} species are present in the framework within a thin surface shell (1.5–2.0 nm) of ZrO_2 particles when the Zn/Zr ratio is smaller than 1/10; when the ratio is above this, both atomically dispersed Zn^{2+} and ZnO clusters coexist in mixed $Zn_xZr_yO_z$ oxide catalysts. The presence of ZnO clusters shows no significant side effect but only a slight increase of selectivity to CO_2 , caused by steam reforming. The incorporation of atomic Zn^{2+} into the ZrO_2 framework was found to not only passivate strong Lewis acid sites (i.e., Zr-O-Zr) on ZrO_2 , but to also generate new Lewis acid-base site pairs with enhanced Lewis basicity on the bridged O (i.e., $Zr-O^{\ominus}-Zn^{\oplus}$). In the mixed ketone (i.e., acetone and methyl ethyl ketone (MEK)) reactions, while the passivation of strong acid sites can be correlated to the inhibition of side reactions, such as ketone decomposition and coking, the new Lewis acid-base pairs introduced enhance the cascade aldolization and self-deoxygenation reactions involved in olefin ($C_3^{\ominus}-C_6^{\ominus}$) production. More importantly, the surface acid-base properties change with varying Zn/Zr ratios, which in turn affect the cross- and self-condensation reactivity and subsequent distribution of olefins.



1. Introduction

Global demand for olefins is increasing continuously [1,2]. The primary use for lower olefins, such as propylene and butylene, are as chemical feedstocks [3,4]. For example, propylene is used as a building block for chemicals including polypropylene, propylene oxide, and acrylonitrile. Four-carbon olefins (e.g., 1-butene, 2-butene, isobutene) are of interest due to their use in the production of methyl tert-butyl ether (MTBE) and ethyl tert-butyl ether (ETBE) [5]. Five-carbon and C_6 olefins can be blended to form gasoline, alkylated with isobutene to form higher fuel range hydrocarbons, or used as starting material in polymers, fatty acids, mercaptans, and surfactants [6,7]. Traditionally, the primary source of three and four-carbon olefin production has been

from non-renewable fossil fuel resources via naphtha steam cracking. However, there has been much recent interest in finding renewable methods of olefin production due to the concern of diminishing fossil fuel resources [8,9].

Biomass is widely recognized as a primary renewable energy source [10–12]. For lignocellulosic biomass, conversion to hydrocarbons typically is carried out as a multi-step process. One typical example is fast pyrolysis of biomass to yield pyrolysis oil, or bio-oil. This bio-oil is then further converted to hydrocarbon fuels through hydrotreating processes albeit the low carbon yield [11–13]. Significant amounts of small oxygenates like alcohols, carboxylic acids, and ketones can also be derived via pyrolysis of lignocellulosic biomass [12,14]. On the other hand, biomass can also be readily converted to ethanol and acetic acid

* Corresponding authors at: The Gene & Linda Voiland School of Chemical Engineering and Bioengineering, Washington State University, Pullman, WA 99164, USA
E-mail addresses: junming.sun@wsu.edu (J. Sun), yong.wang@pnnl.gov (Y. Wang).

through commercially viable processes, such as fermentation [15]. It can be anticipated that the biomass-derived small oxygenates will be abundant in the near future. With increased availability and decreased cost, achieving effectual catalytic conversion of those small oxygenates (e.g., carboxylic acids, alcohols and ketones) to valuable chemicals like C₃–C₆ olefins is essential to move away from our current dependence on non-renewable fossil resources and finding a renewable and sustainable means to their production.

A crucial step in converting biomass derived components to fuels and chemicals is oxygen removal. Additionally, control over C–C bond formation is necessary to provide the desired hydrocarbon chain length of products [16–20]. Various heterogeneous catalysts have been investigated to convert small oxygenates (e.g., alcohols, ketones, and carboxylic acids) to olefins [21–27]. Direct ethanol dehydration to ethylene has been extensively studied, and advances in this area have been summarized recently [21]. Zeolites (e.g., HZSM-5, LEV zeolite, HSAPO) have been successful in converting small oxygenates commonly found in bio-oil to a mixture of olefins and aromatics [23,28–32]. Their disadvantages include low activity, hard-to-control selectivity between olefins and aromatics, and coke generation that inhibits catalytic activity [23,33]. Conversion of ethanol to propylene has also been reported via a proposed dehydration, polymerization and cracking mechanism over LEV zeolites. These catalysts show both low selectivity and low stability due to fast coking reactions [34,35]. Recently, Iwamoto and coworkers developed a new strategy to selectively convert ethanol to propylene using catalysts such as Ni-M41, Sc/In₂O₃, and Y₂O₃-CeO₂ [22]. The reaction pathway was found to involve ethanol dehydrogenation to acetaldehyde followed by a condensation or ketonization reaction to acetone. The acetone intermediate is then hydrogenated to isopropyl alcohol followed by dehydration that results in a higher selectivity to propylene than what is achievable on traditional zeolite catalysts. For converting carboxylic acids to chemicals ketonization, a bimolecular reaction in which two carboxylic acids couple to form a ketone, is generally used. In this particular case, not only does this reaction achieve C–C coupling to increase the chain-length of the resulting ketone, but ketonization can accomplish oxygen removal, leading to only CO₂ and H₂O as byproducts. This reaction has been well studied over alkaline-earth-metal oxides and transition-metal oxides such as Mn₂O₃-CeO₂, ZrO₂, and TiO₂ [36–38]. A variety of proposed reaction mechanisms exist for this reaction over different metal oxides [39]. In separate works, ketone to olefin conversion has been reported over zeolites, where Brønsted acid sites are considered to be the active sites involved in the reaction, as well as over transition-metal oxides [40–46].

We have recently developed unique Zn_xZr_yO_z mixed-metal oxide catalysts for a cascade ethanol-to-isobutene (ETIB) reaction [47–49]. The Zn_xZr_yO_z mixed-metal oxide catalyst was later found by other groups for direct acetic acid-to-isobutene conversion [50], for upgrading of syngas-derived small oxygenates to produce olefins [51,52], and for catalyzing low-temperature ethanol dehydrogenation reactions [53]. Our recent work into this catalyst revealed that, when compared with Brønsted acid sites, Lewis acid-base site pairs are more durable and selective for the cascade ETIB reaction, especially for acetone-to-isobutene conversion (the rate determining step of the cascade reaction) [47]. Moreover, the mixed-metal oxide catalyst Zn₁Zr₁₀O_z (i.e. possessing a Zn/Zr ratio of 1/10) is also highly active and stable for cascade self- and cross-ketonization, self- and cross-aldolization, and deoxygenation reactions for converting mixed carboxylic acids (e.g., mixed acetic acid and propanoic acid) into C₃–C₆ olefins [25,54,55]. More recent work by other groups also suggests that the redox properties of mixed-metal oxides could play key roles in some of the elementary steps of the cascade ETIB reactions (e.g., dehydrogenation and ketonization) [56,57]. It should be noted that despite insight gained in the above-mentioned studies on Zn_xZr_yO_z mixed-metal oxide catalysts, the specific Zn²⁺ structure (i.e., Zn²⁺ location and degree of dispersion) and its effect on the surface chemistry (e.g., Lewis acid-base

properties) of the catalyst remain unclear, and whether this surface chemistry affects the cross-condensation of the mixed acid feed is yet to be explored. Through this work, by using complimentary characterizations such as nitrogen sorption, XRD, XPS, visible Raman, STEM, NH₃-TPD, CO₂-TPD, Py-IR, and CO₂-IR, we have further identified the surface structure and functionality of Zn_xZr_yO_z mixed-metal oxide catalysts with varied Zn/Zr ratios. In particular, we report findings on the structure of Zn²⁺ species and its effect on the acid-base properties of the catalyst surface. The rate-determining mixed ketone reactions (acetone and methyl ethyl ketone), for simplicity, were mainly used to investigate how the surface acid-base properties affect the self- and cross-aldolization and self-deoxygenation of ketones, which effectively control the product distribution of C₃–C₆ olefins.

2. Experimental

2.1. Materials and catalyst synthesis

Zr(OH)₄ (MEL, XZO631/01), Zn(NO₃)₂·6H₂O (Sigma-Aldrich, reagent grade, 98%), ZnO powder (Sigma Aldrich), Methyl ethyl ketone (MEK, 99.7%), Acetone (J.T. Baker, 99.8%), Pyridine (J.T. Baker, 100%). The Zn_xZr_yO_z catalysts (x, y, and z represent the molar ratio of each component) were synthesized via incipient wetness impregnation using Zr(OH)₄ (MEL, XZO631/01) as the support. Briefly, the Zr(OH)₄ powder was dried at 105 °C overnight before impregnation with Zn(NO₃)₂·6H₂O (Sigma-Aldrich, reagent grade, 98%) precursor solution. The concentration of the solution was adjusted to achieve the desired Zn/Zr ratio. After drying this mixture at room temperature overnight and then at 105 °C for 4 h, it was then heated to 400 °C at 3 °C/min and calcined at this temperature for 2 h. The samples were then heated to 550 °C at 5 °C/min and calcined at this temperature for 3 h. ZrO₂ samples were prepared via calcination of Zr(OH)₄ in air following the same calcination procedure described above.

2.2. Characterization

Specific surface areas of the catalysts were determined via nitrogen sorption experiments carried out on a Micromeritics TriStar 2 3020 physisorption analyzer. Catalyst samples were degassed at 350 °C for 3 h under vacuum before experiments were carried out at a temperature of –196 °C.

The bulk phases of the Zn_xZr_yO_z samples were analyzed by X-ray diffraction. The diffractograms were recorded on a Rigaku Miniflex 600 apparatus using Ni-filtered Cu Kα radiation (λ = 0.15406 nm). For each sample, Bragg's angles between 10° and 90° were scanned at a rate of 1.4°/min.

XPS measurements were performed with a Physical Electronics Quantera Scanning X-ray Microprobe. This system uses a focused monochromatic Al Kα X-ray (1486.7 eV) source for excitation and a spherical section analyzer. The instrument has a 32 element multi-channel detection system. The X-ray beam is incident normal to the sample and the photoelectron detector is at 45° off-normal. High energy resolution spectra were collected using a pass-energy of 69.0 eV with a step size of 0.125 eV. For the Ag 3d_{5/2} line, these conditions produced a FWHM of 1.0 eV ± 0.05 eV. The binding energy (BE) scale was calibrated using the Cu 2p_{3/2} feature at 932.62 ± 0.05 eV and Au 4f_{7/2} at 83.96 ± 0.05 eV. Low energy electrons at 1 eV and 20 μA, and low energy Ar⁺ ions were used to minimize the charging effect on the samples analyzed. Quantification was performed using standard sensitivity factors contained in the ULVAC-PHI, Inc. MultiPak software V9.6.1.7 dated October 2016. Peak area intensities required for quantification were calculated after applying Shirley background subtraction to the data. These quantification results include the instrument transmission function, source angle, and asymmetry corrections.

Transmission electron microscopy (TEM) imaging was performed on a FEI Titan 80–300 operated at 300 kV. The images were acquired with

Download English Version:

<https://daneshyari.com/en/article/6498314>

Download Persian Version:

<https://daneshyari.com/article/6498314>

[Daneshyari.com](https://daneshyari.com)